Analysis of the Disorder Occurring in the Crystal Structure of Syndiotactic Polypropylene

Finizia Auriemma, Claudio De Rosa,* and Paolo Corradini

Dipartimento di Chimica, Università di Napoli Federico II, via Mezzocannone 4, 80134 Napoli, Italy

Received March 8, 1993; Revised Manuscript Received June 11, 1993[⊗]

ABSTRACT: Some possible kinds of disorder in the packing of chains of syndiotactic polypropylene, compatible with the maintenance of crystalline long-range order, are discussed and the corresponding models are described. The diffraction intensities at appropriate points or lines of the reciprocal lattice are calculated for the various models; experimental observations of the intensity lowering of some reflections and the appearance of haloes are explained with the models in a semiquantitative way. The possible connection of some kinds of disorder with the presence of configurational defects along the chains is discussed.

Introduction

The occurrence of polymorphism and statistical disorder in the crystal packing of syndiotactic polypropylene (s-PP) has been detected in uniaxially oriented specimens,[1,2] in polycrystalline samples,[2,3] and in single crystals.[4,5]

It has been proposed[6] that the polymorphic behavior and the crystalline disorder are related to the following: the helices s(2/1)2 of s-PP—right and left handed—have an almost identical outside envelope. In relation to the degree of stereoregularity of the polymer and to the crystallization conditions, the helical chains may end up, on crystallization, being packed more or less disorderly according to one of two base main models, represented in Figure 1.

The position of the chain axes, the orientation around the axes, and the relative height of the carbon atoms of the methyl groups of neighboring macromolecules characterize the two basic models of the mode of packing of the methyl groups: (Figure 1A) B-centered (axes in 0, 0, z and $^1/_2$, 0, z); (Figure 1B) C-centered (axes in 0, 0, z and $^1/_2$, $^1/_2$, z); identical a, b, c axes.

The purpose of this paper is to calculate the effect on models of various types of order–disorder (for instance in the relative chirality of neighboring macromolecules) on the diffraction patterns of the polymer samples.

Model Structures for the Calculations

Let us take into consideration idealized models of possible crystalline structures of syndiotactic polypropylene (s-PP), having various degrees of order.

The considered modes of packing of the chains (with *ideal* periodic repetition s(2/1)2) may be classified in terms of the structural features for which long-range positional order is maintained and in terms of the structural features for which only short-range positional order is maintained instead.[7]

We shall refer to structures having the following periodicities:

(i) $c' = 7.40$ Å along the chain axis: this long-range periodicity may refer to all the carbon atoms of a polymer chain (with s(2/1)2 symmetry) or only to the position of the carbon atoms of the methyl groups, belonging to right-handed or, vicariously, to left-handed chains.

(ii) $b' = 5.60$ Å for the chain axes of neighboring chains, as a result of the interdigitation and close packing of touching methyl groups, with a shift of $1/2c$:[6] this gives rise to bc planes (layers) of macromolecules.

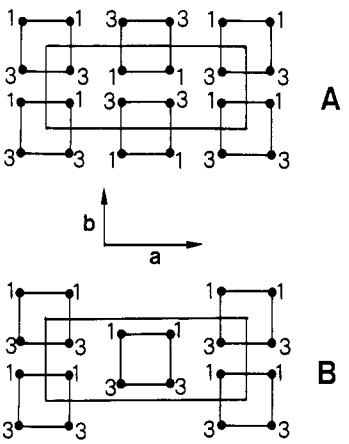

Figure 1. Model of packing of helices in the a–b plane: in a B-pseudo-centered structure (A); in a C-pseudo-centered structure (B). The relative heights of the methyl groups at the vertices of approximate squares are indicated in $c/4$ units.

(iii) $a' = 7.25$ Å for the distance between bc layers, piled one on top of the other and stacked with faults (the chain axes maintaining however their parallelism among themselves) or according to a regular pattern.

We shall designate as "limit ordered structure" an idealized description in a given space group, resulting in a fixed position for all the (carbon) atoms in the crystal; we shall include in the expression "limit disordered structure" an idealized description in a space group, with statistical occupancy of some or all of the equivalent positions.

In crystals with disorder, the concepts of limit ordered structure and of limit disordered structure are both useful.

A limit ordered structure may correspond to the description of the actual relative position of atoms in the short range; its concept may be useful to interpret diffuse X-ray scattering phenomena.

A limit disordered structure may be appropriate for the description of the relative position of atoms in the long range and the occurrence of sharp lines in diffraction experiments.

As an example, useful for the following calculations, we report some ideal models described by Corradini, Napolitano and Pirozzi.[6]

These models have the following:

(1) Perfect three-dimensional order. s-PP ordered crystalline structures have been described according to the limit space group $C222_1$[1] for C-centered structures, where all the helices are of the same hand, and according to the limit space group *Ibca* for the B-pseudo-centered structures, in which helices of opposite hand alternate

[⊗] Abstract published in *Advance ACS Abstracts*, August 15, 1993.

0024-9297/93/2226-5719$04.00/0

regularly along both the axes a and b (with the result that the b axis is twice the value of b').[3,8] For the B-pseudo-centered structures another possibility has been described, arising from the assumption of bc layers built up of isochiral helices while helices facing one another along a are regularly of opposite hand. The space group would be $Pca2_1$[4] (alternatively $Pcaa$ if the full symmetry of the chain is maintained[2]).

(2) Perfect three-dimensional order only for the positions of the axes of the helices. These structures correspond to models, where right- and left-handed helices may substitute each other (i) with complete statistical disorder (corresponding to the limit space group $Cmcm$ in the case of C-centered structures, $Bmcm$ in the case of B-pseudo-centered structures)[2] or alternatively (ii) with preservation of local correlations, as far as the chirality of neighboring chains is concerned. Very simple models (where disorder develops along one direction only) are as follows.

In the case of a C-pseudo-centered structure, the helical chains belonging to the same bc layers may be supposed to be isochiral, while those belonging to adjacent layers (along a) have a probability p of maintaining the same chirality and a probability $1-p$ of being of opposite chirality; in the case of a B-pseudo-centered structure, the helical chains may be supposed to have opposite chirality regularly along b and to repeat along a with a probability p of being of opposite chirality and $1-p$ of being isochiral; or, else, the helical chains may be supposed to have the same chirality regularly along b and to repeat statistically along a with a probability p of being of opposite chirality and $1-p$ of being isochiral.

It is worth noting that a disorder in the stacking of layers of macromolecules has been proposed also for isotactic polypropylene.[9,10]

(3) Bidimensional (long-range) order for the position of the chain axes and the pendant methyl groups; disorder in the stacking of layers. A very simple model of this kind may consist of a statistical mixing, within the same crystal, of C- and B-pseudo-centered structures. In other words, consecutive bc statistical layers may be related by two possible translation vectors: $\mathbf{t}_1 = \mathbf{a}/2 + \mathbf{c}/2$ (like in a B-pseudo-centered structure) or $\mathbf{t}_2 = \mathbf{a}/2 + \mathbf{b}/2$ (like in a C-pseudo-centered structure), with equal or different probabilities.

It has been calculated that the energies for all these structures are comparable, in accordance with our statement that right- and left-handed helices of s-PP have an almost identical outside envelope.[6] Whether right or left-handed, the helices are closely intergiditated along b, scarcely along a;[6] accordingly, we assume that more or less ordered structures are feasible, as a result of the chemical and physical history of the sample.

Limit disordered structures like those represented by statistical space groups such as $Cmcm$ or $Bmcm$ imply that chains of opposite handness may be found (at chance, at least in the long range) around any given axis. This poses the question, whether each single macromolecular chain may take successively right- and left-handed helical conformations along one given axis, while maintaining a correlation in the position of the methyl groups (as shown in Figure 2A).

In Figure 2A, it is assumed that the two portions of the chain (the left- and right-handed ones) on both sides of conformational inversion (indicated with a question mark) remain coaxial. At the same time the positions of the methyl groups belonging to these two portions, a few atoms beyond the defect, are at the proper positions to be well interdigitated with those of adjacent chains, at a low cost of free energy.

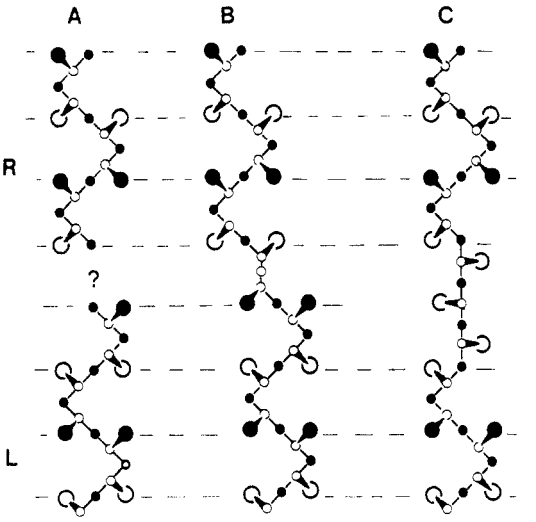

Figure 2. (A) Schematic drawing of the left- (L) and right-handed (R) portions of s-PP chains. The two portions are assumed to be coaxial; the methyl groups are in register with the crystallographic positions on both sides of the conformational inversion (indicated by a question mark). (B) The conformational inversion corresponds to an inversion in the succession of configurations (configurational defect of the kind *rrrrmrrrr*). (C) The conformational inversion occurs in the absence of inversion in the succession of configurations, through the "vacancy" of a monomeric unit.

A conformational inversion, of the kind in Figure 2A, may occur correspondingly to configurational defects of the kind ...*rrrmrrr*..., as shown in Figure 2B. Such defects are probably tolerated within the crystals of s-PP.[11]

A conformational inversion, which is not pinned to a configurational defect but which requires instead the vacancy of one monomeric unit, is shown in Figure 2C. The vacancy, if allowed in the crystals, should be probably highly mobile.

Both the examples shown in Parts B and C of Figure 2 are indicative models of point defects in the crystals of s-PP, to be taken as suggestive of a possibility.

In such crystals, however, even in the case that one or more inversions of helix handness are present along each axis, we can always imagine a core which is strongly correlated in the short range and more peripherical parts, in which that precise correlation fades away and (ultimately) disappears.

A possible model of the crystal is shown in Figure 3.

Each crystal may be conceived of as being built up of blocks, in the core of which some kind of short-range order (corresponding to a limit ordered structure) may have been achieved.

At the periphery of the blocks, the higher level of order of the core may fade out (for instance, configurational errors along the chain cause inversions in the sense of spiralization), while the order corresponding to a limit disordered structure is maintained.

The maintenance at a longer range of a lower degree of order (corresponding to a limit disordered structure) may occur within each block and among different blocks within each single crystal.

Experimental Observations and Model Structures

Since the dimensions of the orthorhombic unit cell of s-PP are always $a = 2a'$, $c = c'$, but it may be $b = b'$ or $b = 2b'$, in this paper the indices of reflections are given,

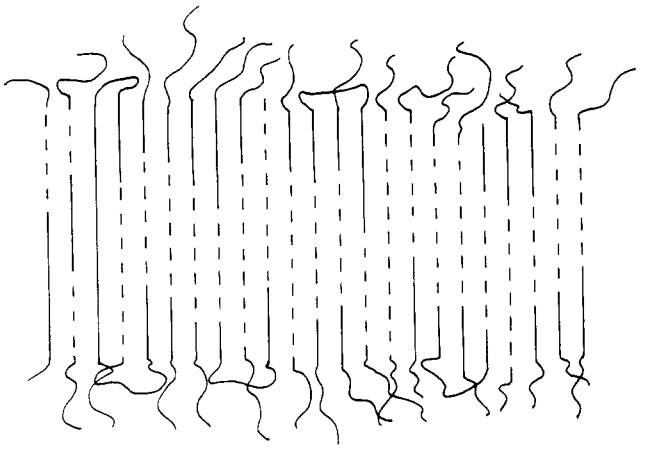

Figure 3. Model of a crystal of s-PP, exemplified in the case of a C-pseudo-centered structure. Helices of opposite handness are indicated by solid and dashed lines. In the crystal there may be a core of helices with identical handness in the short range; in the outskirts the correlation fades away and ultimately disappears.

when necessary to identify univocally the unit cell of reference, using the notation (hkl) $(b = b')$ or (hkl) $(b = 2b')$.

The following kinds of disorder experimentally detected in s-PP samples will be dealt with in this paper:

(A) For C-pseudo-centered structures, the disorder revealed in the case of oriented fiber specimens by the observation that the X-ray diffraction intensity of the (201) $(b = b')$ reflection is weaker than that calculated according to the space group $C222_1$.[1,2] Correspondingly, some diffuse scattering appears in the vicinity of the (201) $(b = b')$ reflection along the first layer line.[2]

(B) For B-pseudo-centered structures, the disorder shown in the case of well-crystallized powders obtained at high temperatures[2,8] by the observation that the X-ray diffraction intensity of the (211) $(b = 2b')$ reflection is weaker than that calculated for the space group *Ibca*.[2] Moreover, in the case of single crystals grown at low temperatures the electron diffraction patterns show diffuse streaking in the h direction around the position of the (211) $(b = 2b')$ reflection[8] in the reciprocal lattice.

(C) For B-pseudo-centered structures, the disorder revealed in the case of single crystals of s-PP grown at different temperatures[3,5,8] by the observation of the streaking of the (010) $(b = b')$ and (210) $(b = b')$ reflections along the h direction of the reciprocal lattice in the electron diffraction patterns: the streaking decreases with an increase of the temperature of growth of the single crystals.[5,8]

As argued in ref 2 the disorder giving rise to the diffraction phenomena described at points A and B can be ascribed to departures from the fully isochiral packing of helices, for C-pseudo-centered structures, to departures from the regular alternance of right- and left-handed helices along a and b, for B-pseudo-centered structures. The limit space groups *Cmcm* and *Bmcm* (whereby right- and left-handed helices would be randomly mixed) are only approximately suited to explain the X-ray diffraction pattern in the two cases, respectively. Indeed, the space group *Cmcm* implies the complete absence of the (201) $(b = b')$ reflection, while the space group *Bmcm* does not explain the presence of the (211) $(b = 2b')$ reflection.

In order to explain the diffraction phenomena, models will be developed, where local correlations in the chirality of neighboring chains are present. As a first approximation in this paper, the disorder will be thought to occur along one direction only (see, for instance, point 2 of the preceding section).

As for the kind of disorder described at point C, it has been argued in ref 5 that a possible model (only bidimensionally ordered) able to explain the experimental pattern is that one described at point 3 of the preceding section.

These simplified models, with disorder occurring along one lattice direction only (i.e., along a), have the advantage of being easily tractable mathematically, in order to evaluate the X-ray diffraction behavior. They are in accordance with the narrowness of the streaks along the b^* reciprocal lattice direction in the electron diffraction patterns.

The evaluation of the diffraction intensities from monodimensionally disordered structures has been abundantly treated in the literature (see refs 12–14 and references therein). In the following sections, we will adapt some of the methods found in the literature, in order to evaluate the X-ray diffraction intensity along the reciprocal lattice lines $(h01)$ $(b = b')$, $(h10)$ $(b = b')$, and $(h11)$ $(b = 2b')$ (h continuous). In all cases the bc layers of helices are assumed to contain a very large (tending to infinite) number of atoms and to succeed along a, in more or less disordered ways. The number (N) of consecutive bc layers is assumed to be finite and variable.

Simple Modeling of the Disorder in C-Pseudo-Centered Structures, for the Diffraction from the $(h01)$ Reciprocal Lattice Line. Mathematical Approach and Results

The limit ordered structural model of s-PP, first proposed by Corradini et al.[1] (space group $C222_1$), is characterized by the presence of bc layers of isochiral helices, juxtaposed to those adjacent (along a), with a probability $p = 1$ of maintaining the same chirality. At the opposite limit, an ideal ordered structural model of packing of s-PP can be thought of as built up of bc layers of isochiral helices, juxtaposed to those adjacent with a probability $1\text{-}p = 1$ of being of opposite chirality (space group *Pbnn*). It is worth noting that, in the limit ordered space group $C222_1$, $(h01)$ reflections with h = integer and even would be present and those with h = odd absent; in the limit ordered space group *Pbnn*, $(h01)$ reflections with h = integer and even would be absent and those with h = odd present.

We consider now a model with disorder, where each bc layer of the isochiral helices is juxtaposed to the neighboring one with a probability p of maintaining the same chirality and $1\text{-}p$ of being of opposite chirality.

The bc layers repeat with translation vector $^1/_2\mathbf{a} + {}^1/_2\mathbf{b}'$; their number is N. The problem of the calculation of the X-ray diffraction intensity from a system such as that described above has been treated in a general form by Hendricks and Teller,[12] and we have adapted their treatment to our case.

Structure factors $V^{(1)}$ and $V^{(2)}$ which are complex conjugate may be associated to the two considered layers of opposite chirality. They are functions of the reciprocal vector, $\mathbf{S}$ (having modulus $(2 \sin \theta)/\lambda$), and of the coordinates of the atoms in a layer. The choice of the origin of the system of axes associated to the layers places the carbon atoms in the lattice positions indicated in Table I; the structure factors associated to the layers have the real part equal to zero so that $V^{(1)} = -V^{(2)} = iB$. The introduction of the physical quantities as defined above

Table I. Fractional Coordinates of the Carbon Atoms of an Asymmetric Unit of s-PP[a]

		$x = X/a$	$y = Y/b'$	$z = Z/c$	occupation factors
C_1	(CH_2)	0.000	0.010	0.250	1/2
C_2	(CH)	0.061	0.165	0.385	1
C_3	(CH_3)	0.122	0.331	0.241	1
C_4	(CH_2)	0.121	0.000	0.500	1/2

[a] The fractional coordinates of the atoms of a whole chain with s(2/1)2 symmetry are x, y, z; $x, -y, -z$; $-x, -y, z-1/2$; and $-x, y, 1/2 - z$.

in eq 1 of ref 12 gives for the average square of the modulus of the structure factor of the system of N layers (the calculated diffracted intensity):

$$|F(\mathbf{S})|^2_{av} = \sum_{m=1}^{N}\sum_{m'=1}^{N}|(V^{(1)} + V^{(2)})/2|^2 \exp(2\pi i(m-m')\mathbf{t}\cdot\mathbf{S}) + \sum_{m=1}^{N}\sum_{m'=1}^{N}(2p-1)^{|m-m'|}|(V^{(1)}-V^{(2)})/2|^2 \exp(2\pi i(m-m')\mathbf{t}\cdot\mathbf{S}) \quad (1)$$

After some algebraic transformations, we get

$$|F(h01)|^2_{av}/N = B^2[1 + 2/N\sum_{q=1}^{N-1}(N-q)(2p-1)^q \cos(\pi q h)] \quad (2)$$

For N tending to infinity eq 2 reduces to:

$$|F(h01)|^2_{av}/N = B^2[1 + (2p-1)^2]/[1 + (2p-1)^2 - 2(2p-1)\cos(\pi h)] \quad (3)$$

which holds only for $p \neq 0$ and $p \neq 1$.[13]

For an ordered structure with all layers of helices having the same chirality, p is equal to 1 (all layers are of the same kind). On the contrary, for an ordered structure where layers of helices of opposite chirality alternate along a, p is equal to 0. In the calculations, the atomic scattering factor of the carbon atom for X-ray has been taken in ref 15.

Figure 4 compares the calculated values of $|F(h01)|^2_{av}/N$ vs h around $h = 2$ for p = 1, $N = 50$ (Figure 4A), $p = 1$, $N = 20$ (Figure 4B), $p = 1$, $N = 10$ (Figure 4C), $p = 0.9$, $N \geq 20$ (Figure 4D). When $p = 1$ (cases A–C), the lower N is, the higher the half-width of the peak is (which is in fact approximately proportional to $1/N$). When p is different from 1, the half-width is on the order $1/(1-p)$ when $N > 1/(1-p)$ (compare Figure 4C, for $p = 0.9$, $N \geq 20$, and Figure 4D, for $p = 1$, $N = 10$). It is worth noting that when statistical disorder is present ($p \neq 1$ and $p \neq 0$), the calculated value of the diffracted intensity along the reciprocal line (h01) is almost insensitive to the value of N, until the case N is infinite, for values of $N > 1/(1-p)$.

A more complete picture of the effect of increasing the degree of disorder is shown in Figure 5, with plots of the diffracted intensity $|F(h01)|^2_{av}/N$ vs h, for $N = 20$ and $p = 1$, 0.9, 0.8, 0.7, 0.6, 0.5 (solid lines), $p = 0$, 0.1, 0.2, 0.3, 0.4 (dashed lines). The higher the degree of disorder, the broader the line profile and the lower the heights of the maxima. In the limiting case $p = 0.5$ (Figure 5F) the curve is very flat.

The results of the calculations performed compare well, qualitatively, with the available diffraction data. The diffuse scattering around the (201) reflection in the first layer line, which is observed in the X-ray diffraction spectra relative to fiber samples of s-PP crystallized in C-pseudo-centered structures,[1,2] can be ascribed indeed to departures from the fully isochiral packing of helices in C-pseudo-centered structures. The model discussed in this section is, however, oversimplified (disordering should not be considered as occurring in one direction only) and can be taken only as a limiting description of the disorder in such s-PP samples.

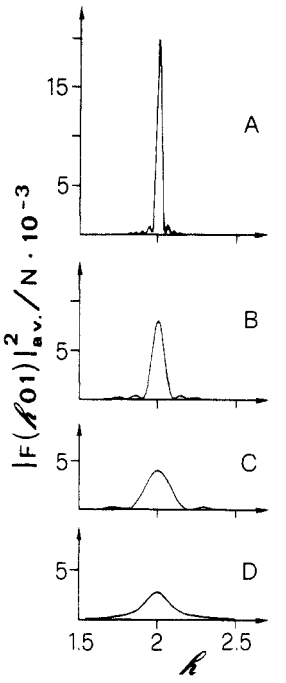

Figure 4. Average square modulus of the structure factor $|F(h01)|^2_{av}/N$ vs h for $p = 1$, $N = 50$ (A); $p = 1$, $N = 20$ (B); $p = 1$, $N = 10$ (C); and $p = 0.9$, $N \geq 20$ (D).

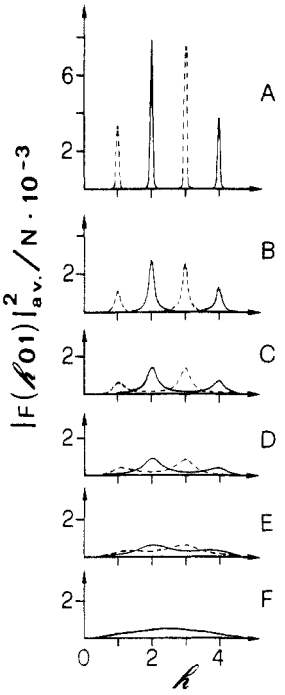

Figure 5. Average square modulus of the structure factor $|F(h01)|^2_{av}/N$ vs h for variable p. Solid lines are for $p \geq 0.5$; dashed lines are for $p < 0.5$. $p = 1$ and $p = 0$ (A); $p = 0.1$ and $p = 0.9$ (B); $p = 0.2$ and $p = 0.8$ (C); $p = 0.3$ and $p = 0.7$ (D); $p = 0.4$ and $p = 0.6$ (E); $p = 0.5$ (F). $N = 20$ for (A); $N \geq 20$ for all other plots.

Possible Modeling of the Disorder in B-Pseudo-Centered Structures for the Diffraction from the (h11) ($b = 2b'$) Reciprocal Lattice Line. Mathematical Approach and Results

In this section we present one of the possible models able to explain the weakness and the broadening of a (211)

($b = 2b'$) reflection, when a strong (020) ($b = 2b'$) reflection is still present, as is observed in the X-ray powder diffraction spectra of some s-PP samples presented in Figures 2a,b and 3b of ref 2.

We suppose that infinite *bc* layers made up of alternating right- and left-handed helices (with structure factors V) are piled along *a*, with a probability *p* that the translation vector is $\mathbf{t}_1 = \mathbf{a}/2 + \mathbf{b}' + \mathbf{c}/2$ and 1-*p* that the translation vector is $\mathbf{t}_2 = \mathbf{a}/2 + \mathbf{c}/2$. As a result, there is a probability *p* that two first neighboring helices, facing along *a*, are of opposite chirality, like in the limit space group *Ibca*, and a probability 1-*p* that these helices are isochiral, like in the limit space group *Bbab*. This case has been mathematically treated in the literature (see, for instance, ref 13 and references therein). In this paper we follow the method given by Allegra in ref 13.

For the simple distribution of probabilities assumed by us, the average square modulus of the structure factor is given by eq 8 of ref 13. In our notation:

$$|F(\mathbf{S})|^2_{av} = NVV^* + VV^* \sum_{q=1}^{N-1}(N-q)\{\overline{[\exp(-2\pi i t\cdot\mathbf{S})]^q} + \overline{[\exp(2\pi i t\cdot\mathbf{S})]^q}\} \quad (4)$$

where *t* corresponds to the translation vector between each couple of consecutive layers and the terms enclosed between braces correspond to the *q*th powers of the factor exp ($\pm 2\pi i t\cdot\mathbf{S}$) averaged over all possible translations between each couple of consecutive layers. These averages are given in our case by:

$$\overline{\exp(\pm 2\pi i t\cdot\mathbf{S})} = (2p-1)\exp(\pm 2\pi i h/2) \quad (5)$$

Hence, for the diffraction along the (h11) ($b = 2b'$) reciprocal lattice line, we have

$$|F(h11)|^2_{av}/N = VV^* + 2VV^*/N\sum_{q=1}^{N-1}(N-q)(2p-1)^q\cos(\pi q h) \quad (6)$$

Similar to eq 2, eq 5 in the limit of *N* tending to infinity reduces to eq 3, which holds only for $p \neq 1$ and $p \neq 0$.[13]

Figure 6 plots the average square modulus of the calculated $|F(h11)|^2_{av}/N$ vs *h* for $N = 20$ and different *p* values. The atomic scattering factor of the carbon atom has been taken for X-ray in ref 15. The diffraction peaks of the ordered structures (Figure 6A) become lower and broader, the higher the degree of the disorder. The same behavior is manifested by the experimental X-ray powder diffraction spectra of samples of highly syndiotactic polypropylene slowly crystallized at high temperature and showing the features of the B-pseudo-centered mode of packing (see Figure 2b of ref 2), where the intensity of the (211) ($b = 2b'$) reflection is almost always lower than that calculated for the limiting space group *Ibca*.[2]

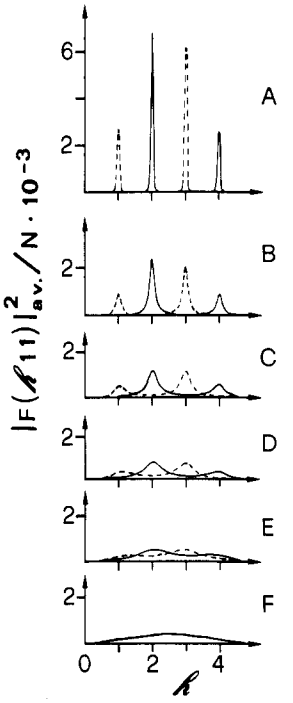

Figure 6. Average square modulus of the structure factor $|F(h11)|^2_{av}/N$ vs *h* for variable *p*. Solid lines are for $p \geq 0.5$; dashed lines are for $p < 0.5$. $p = 1$ and $p = 0$ (A); $p = 0.1$ and $p = 0.9$ (B); $p = 0.2$ and $p = 0.8$ (C); $p = 0.3$ and $p = 0.7$ (D); $p = 0.4$ and $p = 0.6$ (E); $p = 0.5$ (F). $N = 20$ for (A); $N \geq 20$ for all other plots.

Simple Modeling of the Disorder in the Stacking of Chain Axes (Translations $\mathbf{t}_1 = \mathbf{a}/2 + \mathbf{c}/2$ or $\mathbf{t}_2 = \mathbf{a}/2 + \mathbf{b}'/2$) for the Diffraction from the (h10) ($b = b'$) Reciprocal Lattice Line. Mathematical Approach and Results

In the limit ordered structure of s-PP, space group *Pcaa*, proposed by Lotz, Lovinger, and Cais[4] only the (h10) ($b = b'$) reflections with *h* = integer and even are expected to be present, while the (h10) ($b = b'$) reflections with *h* = odd should be absent. On the contrary, in the limit space group proposed by Corradini et al.[1] only the (h10) ($b = b'$) reflections with *h* = integer and odd are expected to be present, while the (h10) ($b = b'$) reflection with *h* = even should be absent. We recall that the layers of helices are piled according to the translation vector $\mathbf{t}_1 = \mathbf{a}/2 + \mathbf{c}/2$, for B-pseudo-centered structures, and to $\mathbf{t}_2 = \mathbf{a}/2 + \mathbf{b}'/2$, for C-pseudo-centered structures.

In this paragraph we evaluate the X-ray diffraction along the (h10) ($b = b'$) layer line for a disordered model where consecutive *bc* layers of helices may be related by the two possible translation vectors $\mathbf{t}_1$ with probability *p* and $\mathbf{t}_2$ with probability 1-*p*. We note that since chains with s(2/1)2 symmetry have centrosymmetric *c* axis projection, *b* can be taken equal to *b'* and the structure factor is the same (the imaginary part is equal to 0), whatever the chirality of the chains is. It is possible to show that the average X-ray diffraction intensity is given by an equation identical to eq 15.

In the calculations, the atomic scattering factor of the carbon atom has been taken for X-ray in ref 5.

Figure 7 plots the calculated diffracted intensity $|F(h10)|^2_{av}/N$ vs *h* for $N = 20$, $p = 1, 0.9, 0.8, 0.7, 0.6$ (solid lines), and for $N = 20$, $p = 0, 0.1, 0.2, 0.3, 0.4$ (dashed lines). Introduction of statistical disorder (*p* different from 0 and 1) produces the lowering and broadening of the intensity maxima, for those peaks of diffraction characteristic of the limiting ordered structures.

It is interesting to compare the family of curves of Figure 7 with the experimental results obtained through the electron diffraction experiments of single crystals of s-PP grown at different temperatures and reported in Figure 2 of ref 5. It is worth noting that the experimental data show a progressive decrease and broadening of the h10 reflections with *h* = even, with decreasing temperature of crystallization of single crystals of s-PP. These trends can be explained with the presence of an increasing degree of disorder of the kind described, within the single crystals. It is worth noting, however, in the experimental case, the progressive appearance of some diffuse maxima around the positions of h10 reflections with *h* = odd, with a

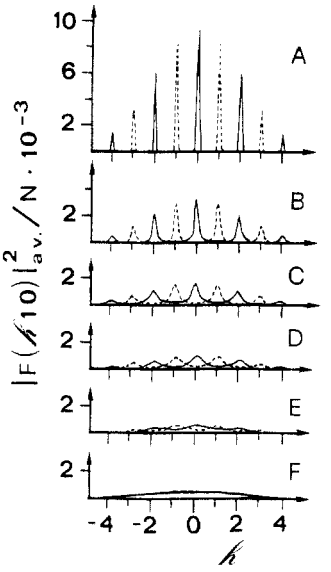

Figure 7. Average square modulus of the structure factor $|F(h01)|^2_{av}/N$ vs h for variable p. Solid lines are for $p \geq 0.5$; dashed lines are for $p < 0.5$. $p = 1$ and $p = 0$ (A); $p = 0.1$ and $p = 0.9$ (B); $p = 0.2$ and $p = 0.8$ (C); $p = 0.3$ and $p = 0.7$ (D); $p = 0.4$ and $p = 0.6$ (E); $p = 0.5$ (F). $N = 20$ for (A); $N \geq 20$ for all other plots.

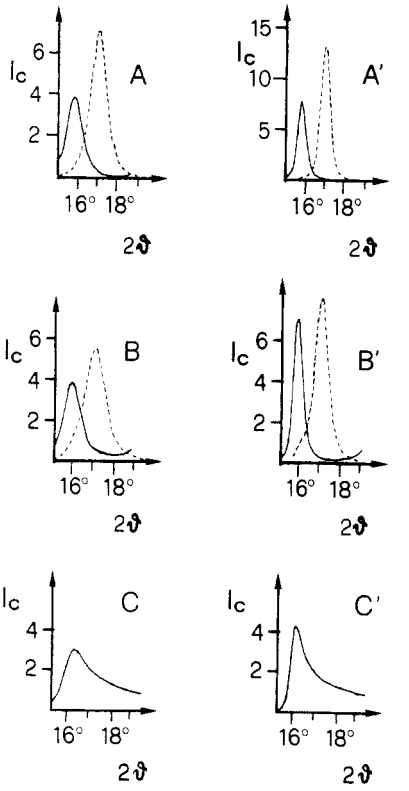

Figure 8. Calculated intensity I_c vs 2θ along the (h10) ($b = b'$) layer line (h continuous) around the positions of (010) ($b = b'$) (solid lines) and (110) ($b = b'$) (dashed lines) reflections (intensity in arbitrary units). $N = 20$, $L_b = 100$ Å, for $p = 1$ and $p = 0$ (A); $p = 0.1$ and $p = 0.9$ (B); $p = 0.5$ (C). $N = 20$, $L_b = 200$ Å, for $p = 1$ and $p = 0$ (A'); $p = 0.1$ and $p = 0.9$ (B'); $p = 0.5$ (C').

decrease of the h10 reflections with h = even. The experimental trends can be explained through our model only by invoking two different statistics, so that the global diffraction pattern experimentally observed for single crystals grown at temperatures less than 100 °C would result as the sum of the contributions due to the presence of two kinds of disorderd crystals: a first kind of crystal would be prevalently B-pseudo-centered ($p > 0.5$) and a second kind prevalently C-pseudo-centered ($p < 0.5$).

In connection with the lowering and the broadening of the (h10) ($b = b'$) reflections with h = even, the same model is able to predict the lowering and the consequent broadening of the (211) ($b = 2b'$) reflection with decreasing p. In this latter case bc layers made up of alternating right- and left-handed helices may be piled along a with probability p that the translation vector is $\mathbf{t}_1 = a/2 + b' + c/2$ and probability (1-p)/2 that the translation vector is $\mathbf{t}_2 = a/2 \pm b'$.

For the simple distribution of probabilities assumed by us, the average square modulus of the structure factor is still given by eq 6 of the preceding section with $(2p\text{-}1)^q$ replaced by p^q.

It is worth noting that the results of the calculations, not reported here, compare well with the experimental electron diffraction data of Lovinger, Lotz, and Davis in ref 8, which indicate that the streaks on the equator (along the (h10) ($b = b'$) layer line) and on the first layer line (along the (h11) ($b = 2b'$) layer line) are related.[8] Indeed the electron diffraction patterns show diffuse scattering along the (h11) ($b = 2b'$) layer line when diffuse scattering is present along the (h10) ($b = b'$) layer line (like, for instance, in the case of single crystals of s-PP grown at 100 °C[8]); they show strong and discrete reflections corresponding to indices (211) ($b = 2b'$) when strong and discrete reflections corresponding to indices (010) ($b = b'$) and (210) ($b = b'$) are present[8] (like, for instance, in the case of single crystals of s-PP grown at 140 °C).

It may be of interest now to compare the calculated X-ray diffraction intensity around the (010) and (110) reflections (corresponding to $2\theta = 15.8°$ and $2\theta = 17.0°$ respectively), in the case of disorder of the kind described above with some experimental data relative to powder X-ray diffraction spectra. To this end, the intensity calculated along the (h10) layer line in the approximation of infinite crystal dimensions along b and c has been smeared out along k, through multiplication with a Lorentzian function, with a maximum for $k = 1$ and a half-width equal to $1/L_b$, with L_b the length of the crystal in the b direction. Hence, the intensity was numerically integrated along circles of constant $S = (2 \sin \theta)/\lambda$, in order to get finally the diffraction intensity as a function of the 2θ diffraction angle. Owing to the equatorial nature of the (h10) ($b = b'$) diffraction line, having not taken into account the finite dimensions of the crystals along c is not very important.

The results are shown in Figure 8. The calculated diffracted intensity vs 2θ is reported for values of $p \geq 0.5$ ($p = 1$, 0.9, 0.5; solid lines) and for values of $p < 0.5$ ($p =$ 0.1, 0; dashed lines). The curves obtained for $L_b = 100$ Å (Figure 8A–C) are compared with those obtained for $L_b = 200$ Å (Figure 8A'–C'). It is apparent that the half-width of the calculated diffracted intensity decreases with increasing the size of the crystal along b. The (110) ($b = b'$) relfection is always broader than the (010) ($b = b'$) reflection in the ordered as well as in the disordered cases. In particular, with increasing L_b, the reflection at $2\theta = 15.8°$ ((010) ($b = b'$)) assumes a characteristic shape, with a steep rise in intensity at low 2θ angle and a slower decrease toward higher angles.[16]

It is known that the experimental X-ray diffraction patterns of powder specimens of s-PP are strongly dependent on the degree of stereoregularity and the thermal history. For instance, we recall from ref 2 that in the case of highly stereoregular polymer (with a content of syndiotactic (*rrrr*) pentads of 94.5%; sample A in ref 2) the X-ray diffraction powder spectra are indicative of a B-pseudo-centered structure, for samples as-polymerized

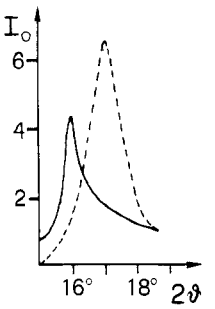

Figure 9. Experimental profile of the X-ray powder diffraction intensity I_0 vs the diffraction angle 2θ, for the s-PP sample designated B in ref 2, in the as-polymerized case (dashed line) and after compression molding (solid line) (intensity in arbitrary units).

as well as for samples slowly crystallized from the melt (cooling rate 1.5 °C/min; compression-molded samples) (see Figure 2 of ref 2). In the case of a less stereoregular polymer of s-PP (with a content of syndiotactic (rrrr) pentads of 88.6%; sample B in ref 2) the X-ray diffraction powder spectrum of the as-polymerized sample is indicative of a C-pseudo-centered structure, while the spectrum of the compression-molded sample (obtained as in the case of sample A) is indicative of a B-pseudo-centered structure (see Figure 3 of ref 2). For sample B we show in Figure 9 the experimental diffraction peak at $2\theta = 17°$ (dashed line) recorded for a sample as-polymerized and the peak at $2\theta = 15.9°$ (solid line) obtained for the sample after compression molding. The general aspect of the two peaks and the comparison with calculated data (see Figure 8) lead us to attribute to the as-polymerized sample prevalently a C-pseudo-centered structure ($1\text{-}p > 0.9$), but low dimensions of the crystallites along *b*, and to the compression-molded sample a high degree of disorder as far as the relative shifts of consecutive *bc* layers along *a* (p around 0.5), but a quite larger dimension of the crystallites along *b*.

Acknowledgment. Financial support from the Ministero dell Università e della Ricerca Scientifica e Tecnologica and from the Progetto Finalizzato Chimica Fine e Secondaria del C.N.R. is gratefully acknowledged.

References and Notes

(1) Corradini, P.; Natta, G.; Ganis, P.; Temussi, P. A. *J. Polym. Sci., Part C* **1967**, *16*, 2477.
(2) De Rosa, C.; Corradini, P. Preceding article in this issue.
(3) Lovinger, A. J.; Lotz, B.; Davis, D. D. *Polymer* **1990**, *31*, 2253.
(4) Lotz, B.; Lovinger, A. J.; Cais, R. E. *Macromolecules* **1988**, *21*, 2375.
(5) Lovinger, A. J.; Davis, D. D.; Lotz, B. *Macromolecules* **1991**, *24*, 552.
(6) Corradini, P.; Napolitano, R.; Pirozzi, B. *Rend. Fis. Acc. Lincei* **1991**, *Vol. II*, 341.
(7) Corradini, P.; Guerra, G. *Adv. Polym. Sci.* **1992**, *100*, 183.
(8) Lovinger, A. J.; Lotz, B.; Davis, D. D. *Polym. Prepr. (Am. Chem. Soc., Div. Polym. Chem.)* **1992**, *33*, 270.
(9) Corradini, P.; Giunchi, G.; Petraccone, V.; Pirozzi, B.; Vidal, H. M. *Gazz. Chim. Ital.* **1980**, *110*, 413.
(10) Bruckner, S.; Meille, S. V.; Petraccone, V.; Pirozzi, B. *Prog. Polym. Sci.* **1991**, *16*, 361.
(11) Ammendola, P.; Shijing, X.; Grassi, A.; Zambelli, A. *Gazz. Chim. Ital.* **1988**, *118*, 769.
(12) Hendricks, S.; Teller, E. *J. Chem. Phys.* **1942**, *10*, 147.
(13) Allegra, G. *Nuovo Cimento* **1961**, *XXI*, 786.
(14) Takahashi, Y.; Tadokoro, H. *Macromolecules* **1983**, *16*, 1880.
(15) Cromer, D. T.; Mann, J. B. *Acta Crystallogr.* **1968**, *A24*, 321.
(16) Wilson, A. J. C. *Acta Crystallogr.* **1949**, *2*, 245.